

INTRODUCTION: 64455 is a basaltic impact melt with a very thick coating of smooth, dark glass (Fig. 1). The basalt is somewhat friable and the bonding between the basalt and the glass coat is generally weak. Along the basalt/glass contact the basalt has been partially melted followed by limited mixing of the melt with the glass coat. The glass coat appears to have once enclosed the entire rock, but a small area on the “lunar top” has been broken away exposing the basalt. Zap pits are present only on the “lunar top” surface. Distinct spheroids and dumbbells of glass are adhering to, and coalescing with, the exterior surface of the coat. This sample was collected from the northeast rim of a subdued crater on the northeast slope of Stone Mountain.



FIGURE 1. S-73-22656.

**PETROLOGY:** Grieve and Plant (1973), Blanford et al. (1974), Schaal et al. (1979) and Vaniman and Papike (1981) provide petrographic information. 64455 is a basaltic impact melt (Fig. 2) with a very thick glass coat. Grieve and Plant (1973) recognize four distinct textural zones within the rock: 1) a crystalline core of basaltic impact melt, 2) a zone of basalt with interstitial partial melt, 3) a thin, discontinuous crust of devitrified glass, and 4) an outer coating of fresh glass.

The basalt consists of ~65% plagioclase ( $An_{90-95}$ , up to 1 mm long) with interstitial low-Ca pyroxene ( $Wo_{6-13}En_{76-68}$ ) which is often cored by minor olivine ( $Fo_{75-80}$ ) (Fig. 3). Accessory metal (Ni 5.1%, Co 0.3%), troilite, schreibersite, and ilmenite account for ~5% of the rock. Several of the melt grains in the basalt are rusty.

Between the core of basalt and the glass coat there is a thin zone (~1 mm wide) of basalt with a significant amount of interstitial glass (Fig. 2). Grieve and Plant (1973) interpret this glass as a partial melt of the basalt, citing as evidence a decrease in the modal abundance of pyroxene, partial resorption of mineral grains, and the complimentary composition of the glass compared to the crystalline residue within this zone. Quench crystals of olivine and pyroxene are common in the interstitial glass and as rims around the partially resorbed grains.

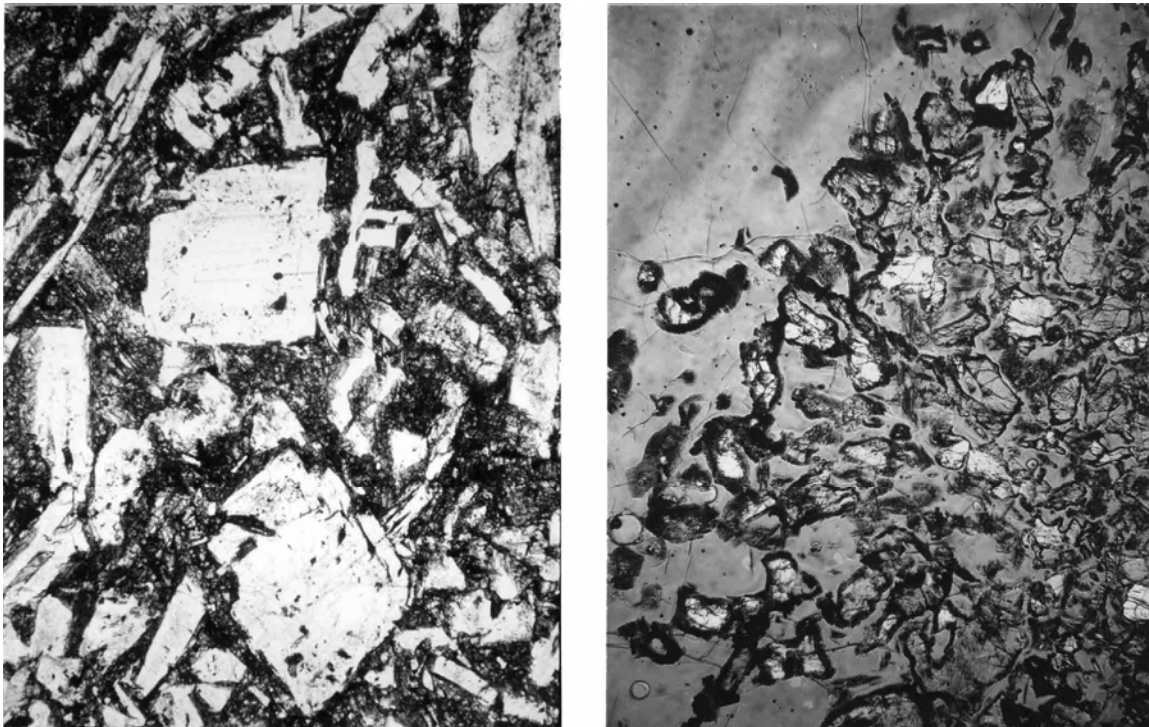


FIGURE 2. a) 64455,70B, basaltic melt, ppl. Width 2 mm.  
b) 64455,38, zone of glass coat, basalt with interstitial melt, ppl. Width 4 mm.

The thin (0.25 mm wide) crust of devitrified glass sandwiched between the basalt and the fresh glass coat contains numerous areas of acicular plagioclase grains and cryptocrystalline mesostasis. As pointed out by Blanford et al. (1974) these are quench crystals and not the products of subsolidus devitrification. This zone is discontinuous and cannot be recognized in every section (Fig. 2). Metal spherules with associated troilite and schreibersite are abundant, as are small vesicles which are concentrated along the basalt/glass contact.

Except for a small eroded area, the fresh glass coat (minimum 2 mm thick) completely encloses the rest of the rock. The smooth external surface of the coat indicates that it formed during free flight. Flow banding is dominantly parallel to the basalt/glass contact and is emphasized by abundant, minute spherules of metal (20.4% Ni, 0.8% Co), troilite, and schreibersite. In contrast to the basalt none of the metal grains in the glass coat are rusty. Swirls of glass around vesicles indicate movement of the melt after emplacement and prior to quenching (Schaal et al., 1979). In several places the glass penetrates the basalt forming veins which occasionally merge with the interstitial partial melt described above. A thin zone of quench crystals is also present along portions of the exterior surface of the coat.

**EXPERIMENTAL PETROLOGY:** Ulrich and Weber (1973) performed differential thermal analyses (DTA) on natural and synthetic samples of the fresh glass coat. The liquidus temperature of the synthetic composition was found to be 1350-1400°C, the solidus temperature is ~1200°C. A cooling rate of 140°C/minute from 1400° was required to match the DTA data on the synthetic composition with that obtained on the natural sample.

**CHEMISTRY:** Major and trace element data for both the basalt and the glass coat are provided by Haskin et al. (1973). Meteoritic siderophile and volatile element abundances for these two lithologies are given by Ganapathy et al. (1974). Grieve and Plant (1973) report broad beam electron microprobe analyses (DBA) of the basalt, the glass coat, glass veins and the interior partial melt. The data are summarized in Table 1 and Figure 4.

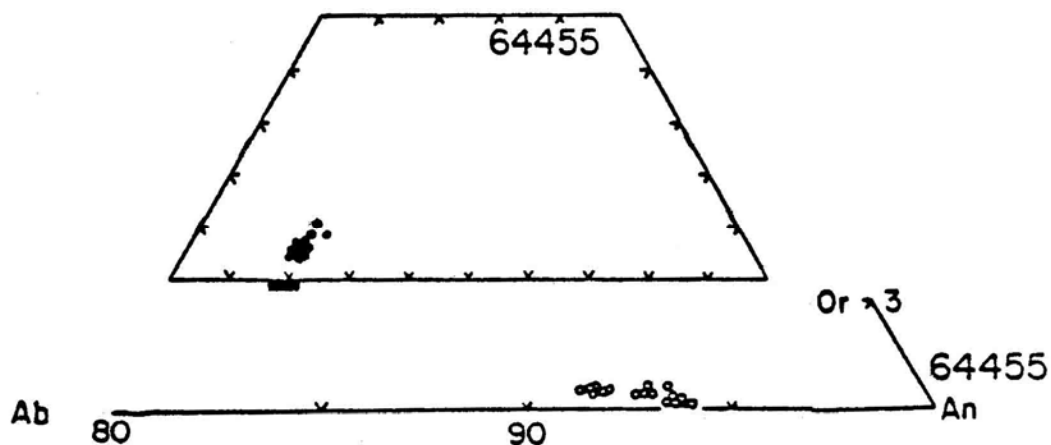


FIGURE 3. a) Mafic mineral compositions, olivine plotted along base.  
 b) Plagioclase compositions, from Vaniman and Papike (1981).

TABLE 1. Summary chemistry of basalt and glass from 64455.

|                                | <u>Basalt</u> | <u>Glass Coat</u> | <u>Partial Melt</u> |
|--------------------------------|---------------|-------------------|---------------------|
| SiO <sub>2</sub>               | 47.8          | 44.1              | 48.6                |
| TiO <sub>2</sub>               | 0.63          | 0.42              | 0.67                |
| Al <sub>2</sub> O <sub>3</sub> | 23.6          | 25.1              | 17.5                |
| Cr <sub>2</sub> O <sub>3</sub> | 0.15          | 0.15              | 0.25                |
| FeO                            | 5.4           | 6.1               | 6.5                 |
| MnO                            | 0.07          | 0.07              | 0.07                |
| MgO                            | 8.5           | 8.0               | 14.0                |
| CaO                            | 13.5          | 14.5              | 11.3                |
| Na <sub>2</sub> O              | 0.43          | 0.36              | 0.84                |
| K <sub>2</sub> O               | 0.22          | 0.08              | 0.26                |
| P <sub>2</sub> O <sub>5</sub>  |               |                   |                     |
| Sr                             |               |                   |                     |
| La                             | 21.1          | 12.6              |                     |
| Lu                             | 0.96          | 0.56              |                     |
| Rb                             | 6.0           | 3.1               |                     |
| Sc                             | 7.8           | 7.0               |                     |
| Ni                             | 80-540        | ~800              |                     |
| Co                             | ~30           | ~50               |                     |
| Ir ppb                         | 2.25          | 40.6              |                     |
| Au ppb                         | 1.56          | 12.7              |                     |
| C                              |               |                   |                     |
| N                              |               |                   |                     |
| S                              |               |                   |                     |
| Zn                             | 3             | 2.4               |                     |
| Cu                             |               |                   |                     |

Oxides in wt%; others in ppm except as noted.

Compared to the crystalline core, the glass coat on 64455 contains more alumina, lower incompatibles, and higher siderophile abundances (Table 1) and thus cannot represent simply a remelt of the basalt. Both the basalt and the glass coat approximate, but do not match, local soil compositions. Grieve and Plant (1973) find that the devitrified glass rim and the glass coat are compositionally identical (Fig. 5) and probably represent textural variations of a single melt. The areas of interior partial melt analyzed by these authors are similar in composition to the KREEP-rich, Apollo 16 poikilitic impact melts (e.g. 60315, 62235) (Table 1). Analyses along a glass vein which connects with the glass coat and penetrates into the partially melted zone show a series of intermediate compositions which span those of the coat and the partial melt (Fig. 5) (Grieve and Plant, 1973).

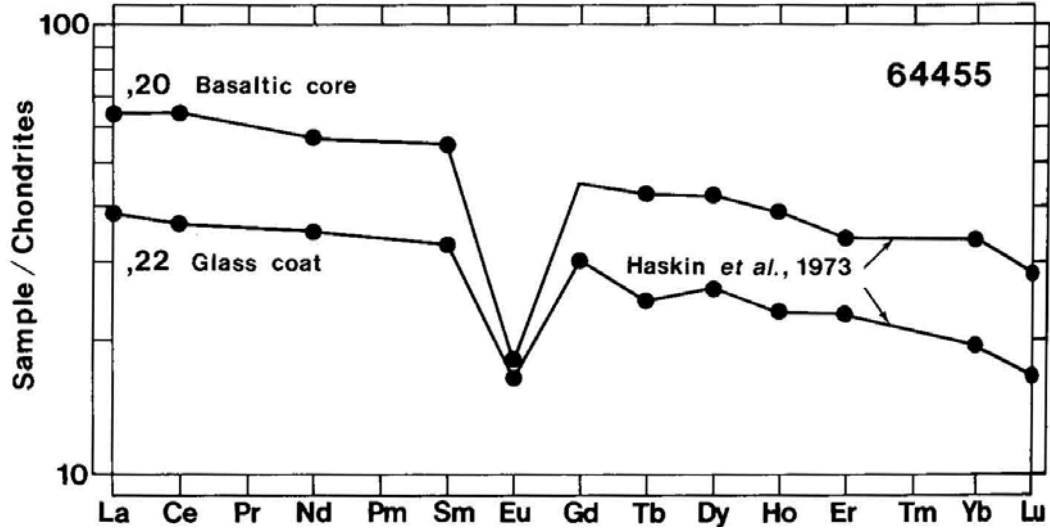


FIGURE 4. Rare earths.

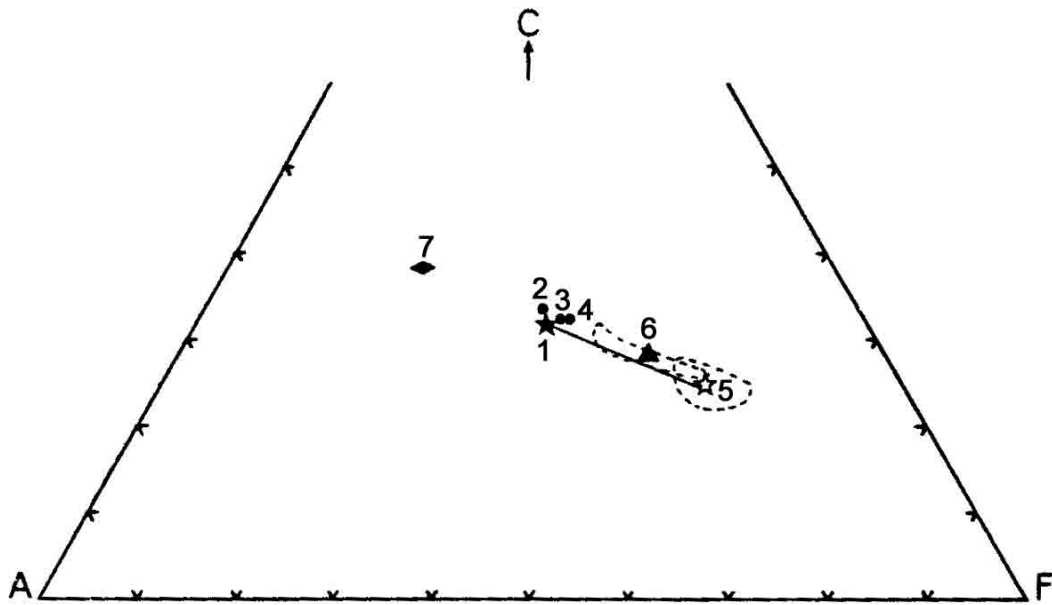


FIGURE 5. Mol.% ACF for various components of 64455,35. The dashed lines show the range of compositions of the partial melt and the glass vein.

- 1) basaltic impact melt. 2) various highland basalt glasses, other authors.
- 3) devitrified rim. 4) glass coat. 5) partial melt. 6) glass vein.
- 7) residual crystalline material in partial melt zone.

From Grieve and Plant (1973).

Hertogen et al. (1977) report different meteoritic groups for the basalt and the glass coat, based on siderophiles. The basalt belongs to meteoritic group 1H, a group largely restricted to the Apollo 16 site. The glass coat contains meteoritic group 5H and is interpreted, along with glass spheres 60095 and 65016, to represent South Ray ejecta (Hertogen et al., 1977).

RARE GAS/EXPOSURE AGES: Bogard et al. (1973) provide He, Ne, Ar, Kr and Xe isotopic data for a chip of basalt. From these data Bogard and Gibson (1975) calculate  $^{21}\text{Ne}$  and  $^{38}\text{Ar}$  exposure ages of 1.2 and 1.8 m.y., respectively. Kr isotopes yielded an exposure age of 2.01 m.y. (Marti, 1975, pers. comm. referenced in Blanford et al., 1975). These low exposure ages and the simple exposure history indicated by microcrater data are consistent with excavation of 64455 by the South Ray cratering event. Blanford et al. (1974) calculate an exposure age of 0.5 - 0.6 m.y. from the microcrater data of Neukum et al. (1973).

MICROCRATERS, TRACKS AND SURFACES: Neukum et al. (1973) provide size-frequency data for microcraters on 64455 (Fig. 6). A simple exposure history is indicated by the fact that only those surfaces exposed at the time of collection have microcraters. The surfaces are in production.

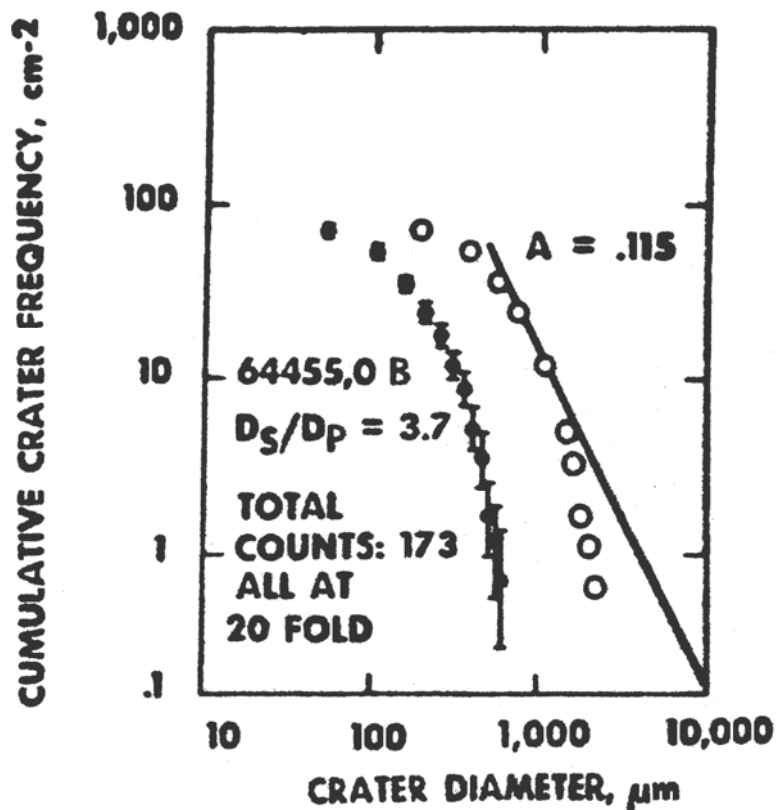
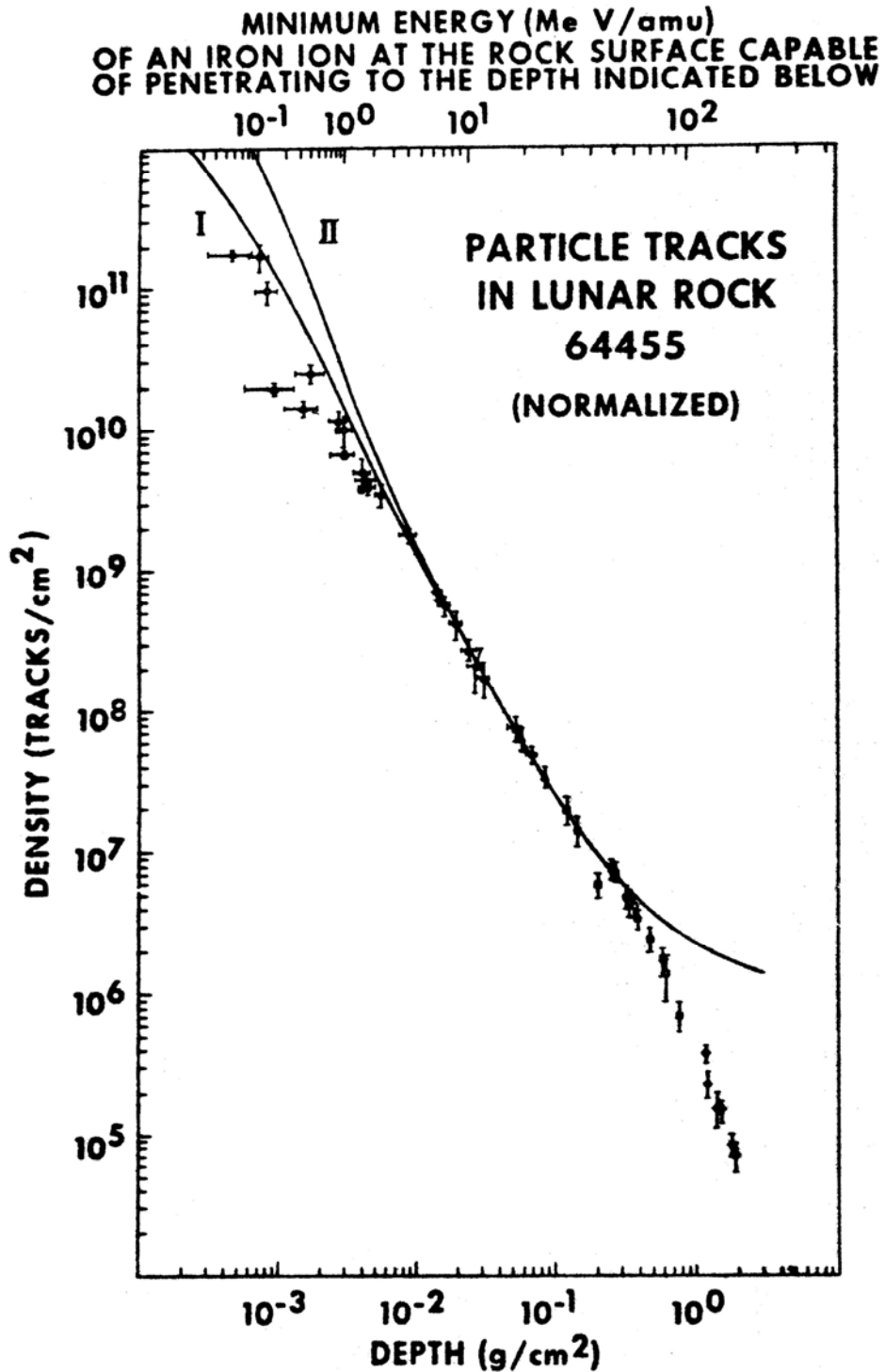


FIGURE 6. Microcraters, from Neukum et al. (1973).

Blanford et al. (1974, 1975) report the particle track profile in the glass coat (Fig. 7) and use the data to discuss the solar energy spectrum.

Leich et al. (1973) determined the depth distributions of H and F in exterior chips of the glass coat and the basalt (Figs. 8, 9). A maximum concentration of H was detected



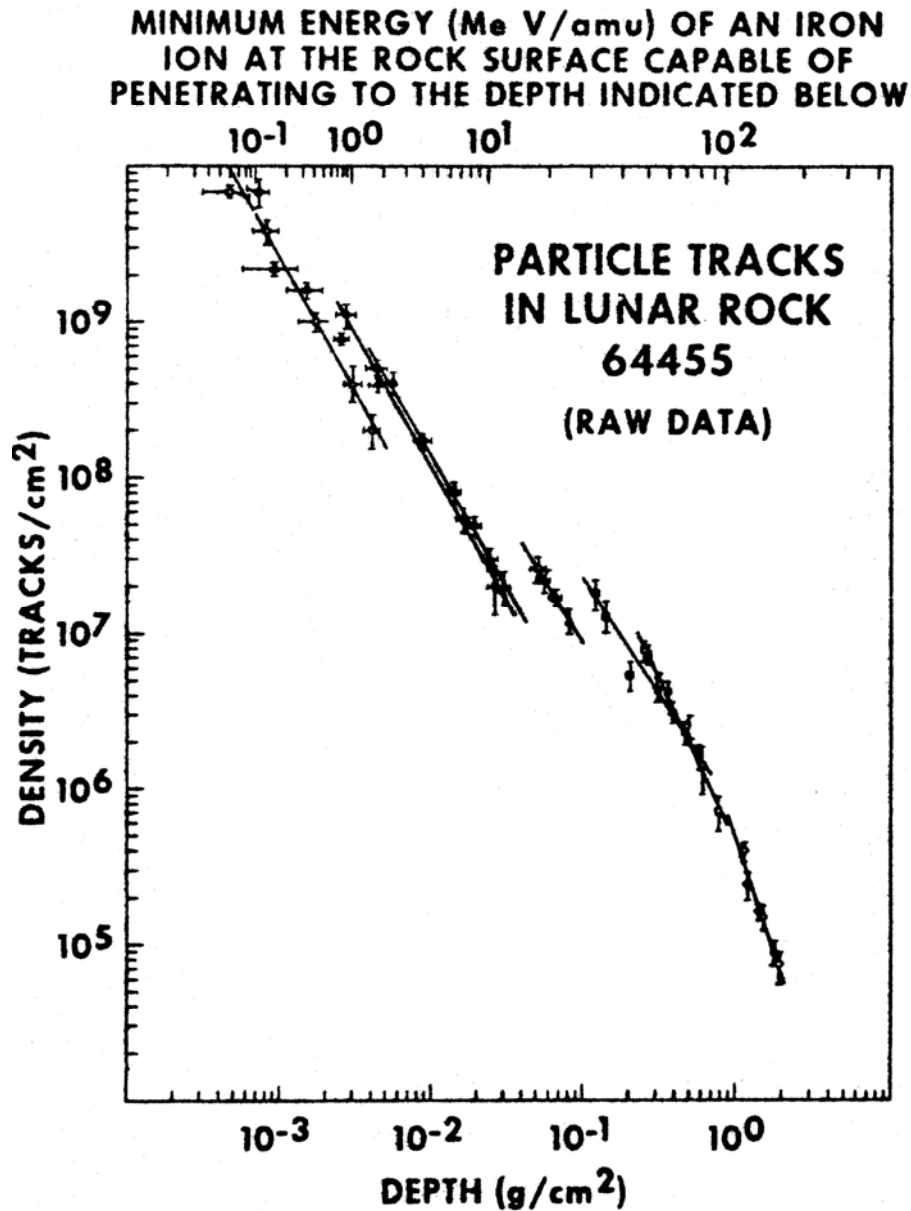
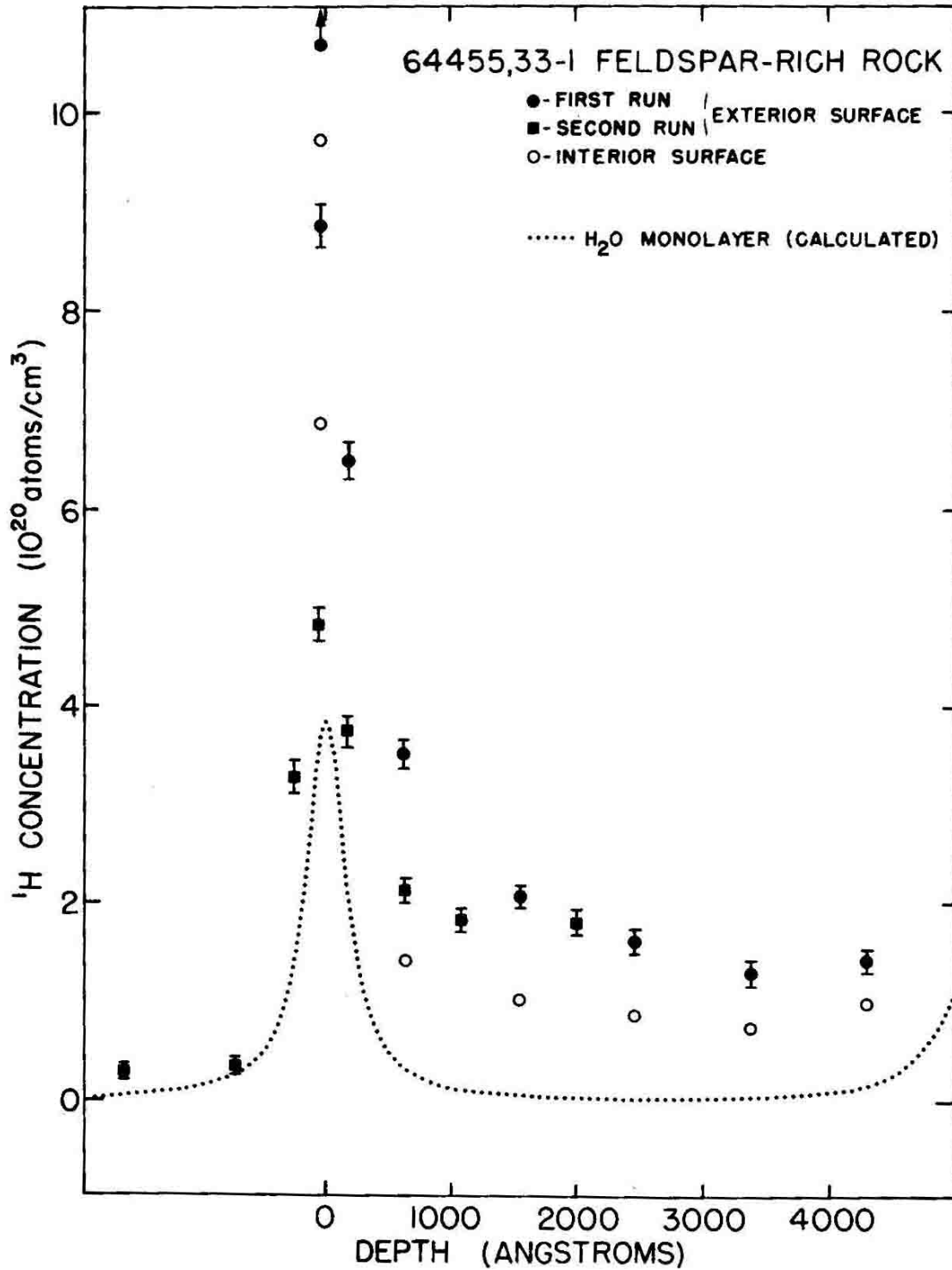


FIGURE 7. Solar flare tracks, from Blanford et al. (1974).

within  $\sim 200 \text{ \AA}$  of the exterior surface of both the rock and the glass chips. As 64455 was exposed to the atmosphere on route to earth and prior to storage in nitrogen-filled cabinets, Leich et al. (1973) consider this H to be terrestrial contamination. The H at  $>2000 \text{ \AA}$  within the basalt and the glass cannot be accounted for by either terrestrial contamination or directly implanted solar wind and therefore was probably inherited from a pre-irradiated component of the impact melt. A peak in the F concentration was observed  $\sim 0.2\text{-}0.4 \text{ \mu m}$  from the exterior surfaces of both the basalt and the glass, but technical problems, poor reproducibility, and the possibility of terrestrial contamination in these samples preclude any judgment as to the origin of the F (Leich et al., 1973).

An upper limit of  $3 \times 10^{15}$  atoms/cm<sup>2</sup> of solar wind implanted carbon for an exterior surface of basalt was reported by Goldberg et al. (1976).



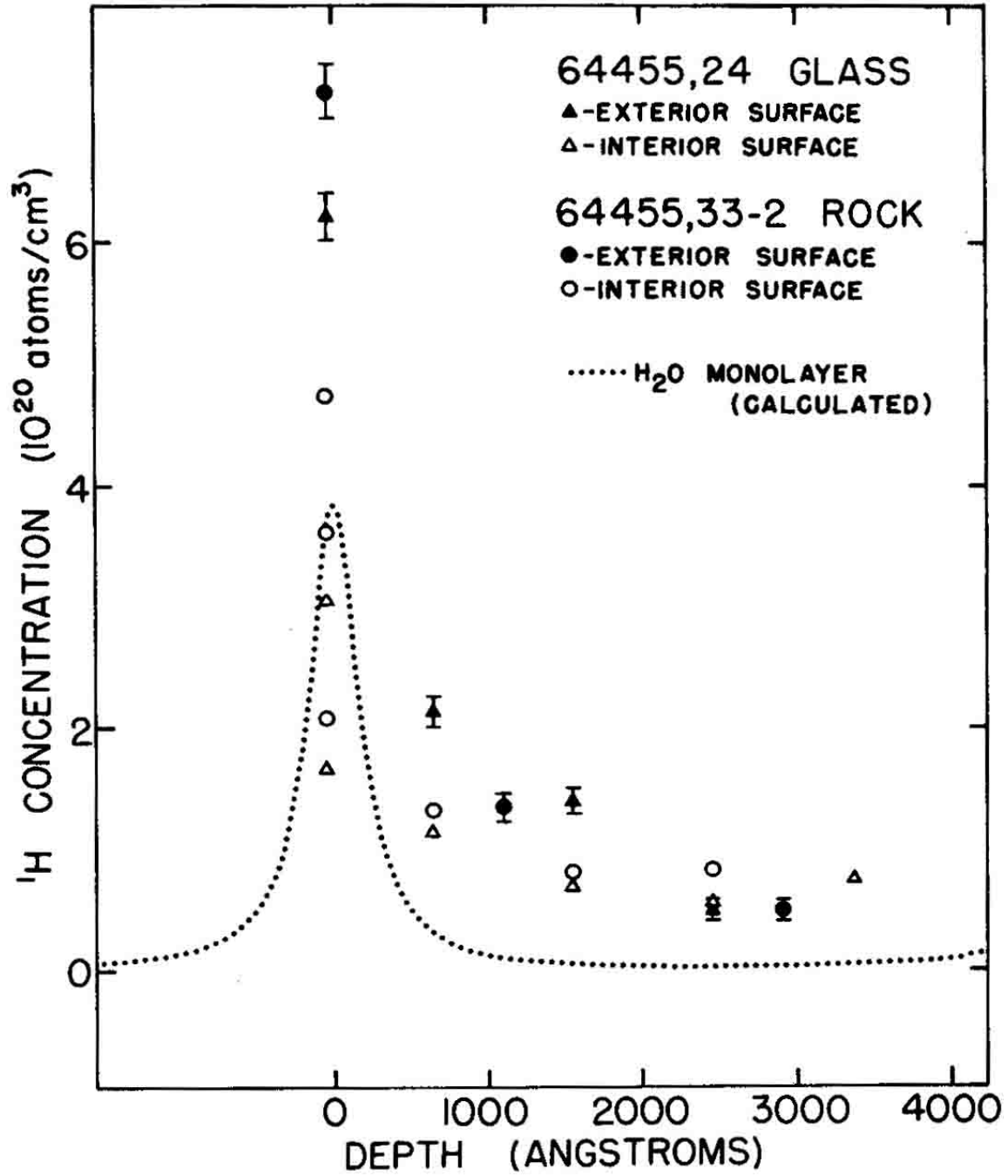


FIGURE 8. Hydrogen concentration v. depth, from Leich et al. (1973).

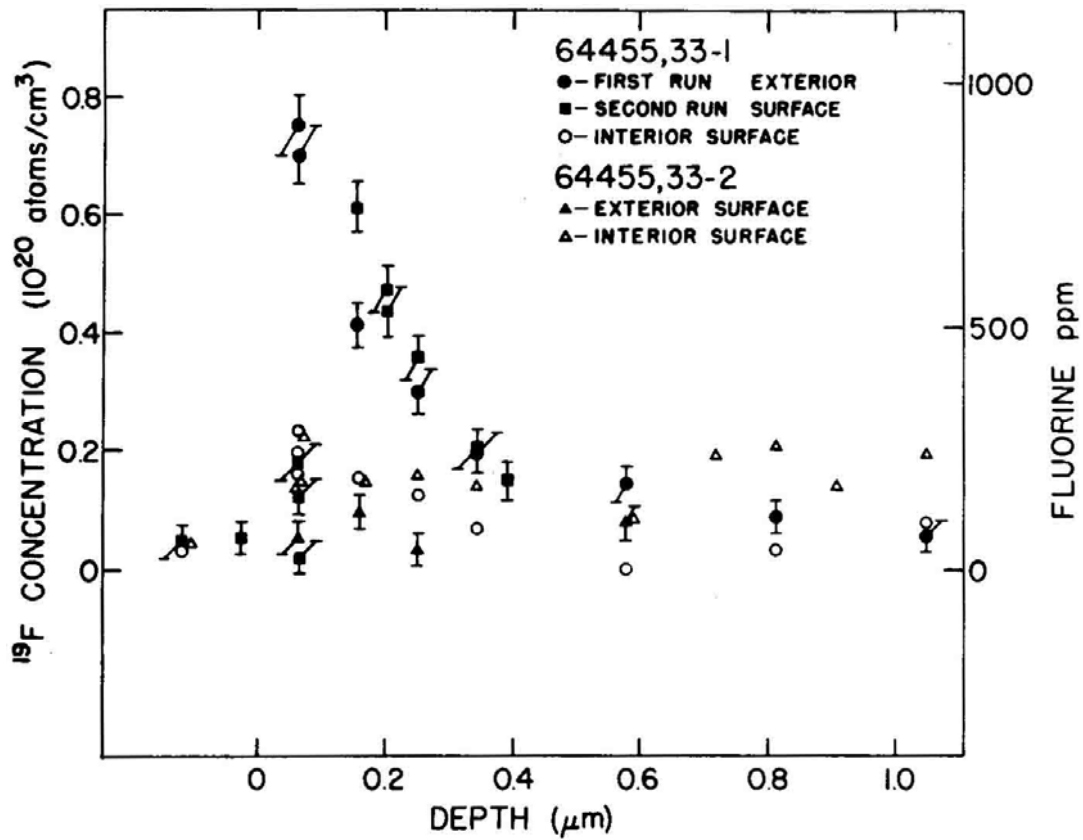
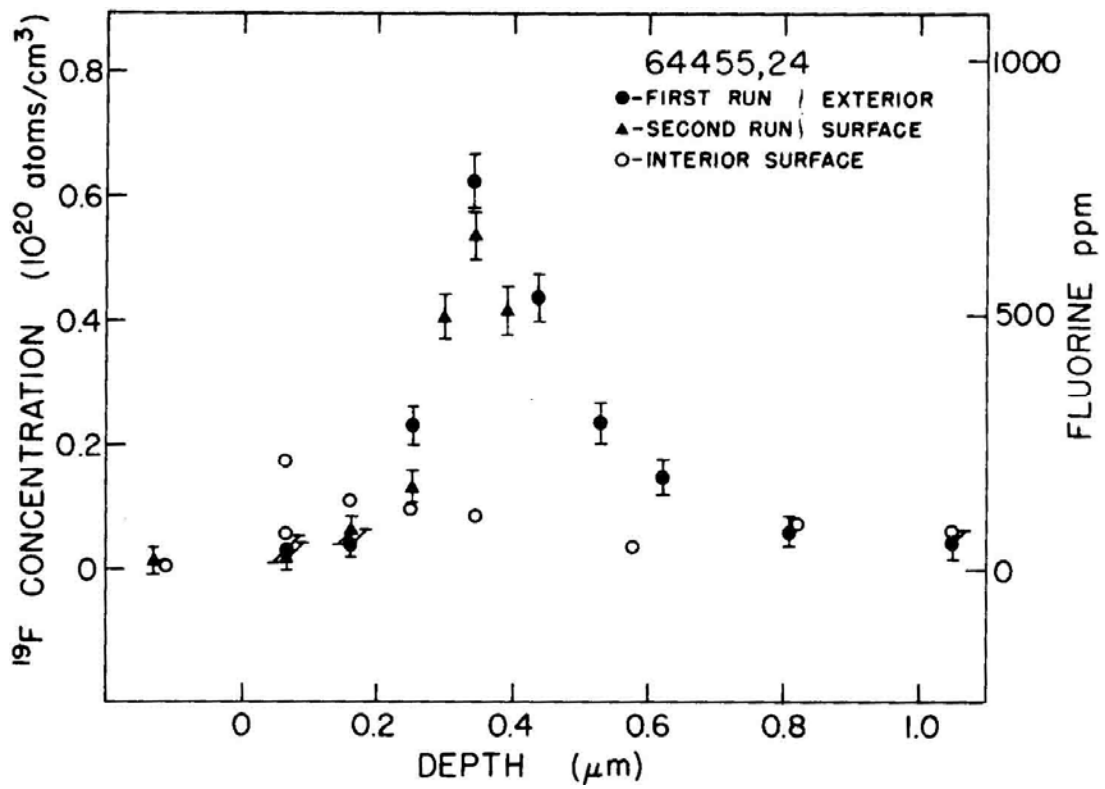


FIGURE 9. Fluorine concentration v. depth, from Leich et al. (1973).

PROCESSING AND SUBDIVISIONS: In 1972, 64455 was cut into three main pieces, including a slab (Fig. 10). The slab was extensively subdivided for allocations. Several chips were also allocated from the Wend of the large butt end (,0).

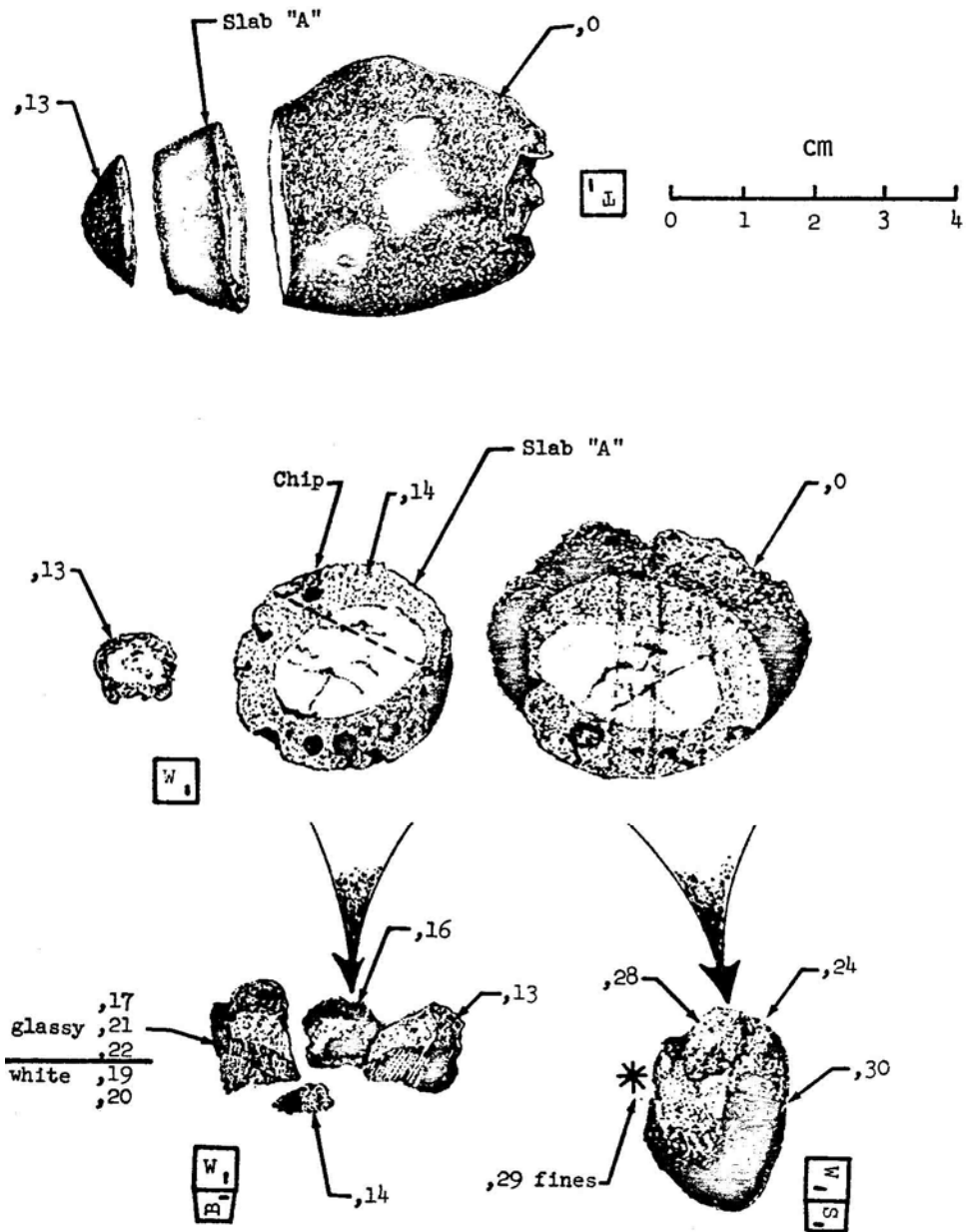


FIGURE 10. Cutting sketch.